Single Electron Transfer and Nucleophilic Substitution. Reaction of Alkyl Bromides with Aromatic Anion Radicals and Low Oxidation State Iron Porphyrins

Doris Lexa, Jean-Michel Savéant,* Khac-Binh Su, and Dan-Li Wang

Contribution from the Laboratoire d'Electrochimie Moléculaire de l'Université de Paris 7, Unité Associée au CNRS No. 438, 2 Place Jussieu, 75251 Paris, Cedex 05, France.
Received March 29, 1988

Abstract: The problem of the role of single electron transfer in S_N2 substitution is discussed on the basis of a comparison of the rate constants obtained for the reaction of alkyl bromides with aromatic anion radicals on one hand and with iron("0") and iron(I) porphyrins on the other, as well as of the temperature dependence of the reaction kinetics. Conceiving S_N2 substitution as an inner-sphere electron transfer, namely, as a single electron transfer concerted with bond breaking and bond formation, the factors that control its occurrence rather than that of a concerted electron transfer–bond breaking process followed by a separate bond-forming step (ET) are identified and discussed. S_N2 tends to be favored over ET since the activation energy is lower owing to bonding interactions in the transition state. This is, however, counterbalanced by a substantially negative activation entropy for the S_N2 pathway as compared to the ET pathway. As a general trend, the ET pathway thus tends to predominate over the S_N2 pathway at high temperatures, and vice versa. Depending upon the strength of the bonding interactions in the transition state, one or the other behavior will usually be observed in the whole accessible temperature range. This is the case with the reaction of iron("0") and iron(I) porphyrins with *n*-BuBr, which occurs along with an S_N2 mechanism. The reaction of anthracene anion radical with *n*-BuBr is a striking borderline case in which the energy–entropy balance passage from an ET to a S_N2 mechanism can be clearly observed upon decreasing temperature. Steric hindrance at the carbon center or at the electron donor reacting center disfavors the S_N2 mechanism making the high activation energy–almost zero activation entropy–ET behavior predominant in most of the investigated temperature range. The analysis of these experimental examples provides the basis for a general discussion of how ET and S_N2 pathways can be distinguished one from the other and of the factors that control the transition between them. It is shown that borderline cases and intermediate mechanisms between ET and S_N2 cannot be conceived in terms of activation energy only but that they can in terms of activation energy–entropy balance provided the angle of attack be taken as an additional reaction coordinate.

The inner-sphere versus outer-sphere character of organic electron transfer reactions has attracted active recent attention, in particular, the role of single electron transfer in carbon-centered S_N2 substitutions. The extension of the outer-sphere/inner-sphere terminology from metal-centered to carbon-centered chemistry[1a] seems now accepted though after some reluctance.[1b,c] For definiteness, let us again specify these two terms: bonds are broken and/or formed concertedly with single electron transfer in inner-sphere electron transfer processes. In outer-sphere electron transfer processes, either bond breaking and/or bond formation do not occur or, if they do, they take place in separate steps preceding or following the electron transfer step. Synonyms of outer-sphere and inner-sphere electron transfers could thus be bond-conserving and bond-changing electron transfers, respectively. Carbon-centered S_N2 substitutions can thus be viewed as inner-sphere single electron transfer reactions[1a] in which a bond is broken and another is formed, both concertedly with electron transfer. In this context, single electron transfer subject to Franck-Condon restrictions provides a more likely description of the reaction, within the framework of the Born–Oppenheimer approximation, than the formally equivalent electron-pair transfer mechanism, since simultaneous extraction of two electrons from the nucleophile appears less probable than extraction of a single electron.[2]

However, several reactions involving the formation of a new bond at a carbon atom have been deemed to proceed in an outer-sphere manner, bond formation taking place in a separate follow-up step. This is the case for the reaction of aliphatic halides with an aromatic or heteraromatic anion radical as the electron donor (nucleophile):[1a,4]

$$RX + D^{\bullet -} \rightarrow D + R^{\bullet} + X^- \quad (1)$$

$$R^{\bullet} + D \rightarrow RD^{\bullet} \quad (2)$$

(followed by: $RD^{\bullet} + D^{\bullet -} \rightarrow RD^- + D$)

or more likely:

$$R^{\bullet} + D^{\bullet -} \rightarrow RD^- \quad (3)$$

(1) (a) Lexa, D.; Mispelter, J.; Savéant, J-M. *J. Am. Chem. Soc.* **1981**, *103*, 6806. (b) Eberson, L. *Electron Transfer Reactions in Organic Chemistry*; Springer-Verlag: Berlin, 1987; pp 14–16. (c) Eberson, L. *Acta Chem. Scand., Ser. B* **1982**, *36*, 533.

(2) (a) Still another terminology, "electron shift",[2b-d] is being used for characterizing these reactions. Inner-sphere electron transfer, i.e., single electron transfer with partial bond breaking and partial bond formation in the transition state, is a formally equivalent concept that may be more suited to a quantitative description of the kinetics of the reaction as an extension of the existing theories of outer-sphere electron transfers such as Hush–Marcus theory.[3] (b) Pross, A. *Adv. Phys. Org. Chem.* **1985**, *21*, 99. (c) Shaik, S. S. *Prog. Phys. Org. Chem.* **1985**, *15*, 197. (d) Pross, A. *Acc. Chem. Res.* **1985**, *18*, 212.

(3) (a) Hush, N. S. *J. Chem. Phys.* **1958**, *28*, 962. (b) Hush, N. S. *Trans. Faraday Soc.* **1961**, *57*, 557. (c) Marcus, R. A. *J. Chem. Phys.* **1956**, *24*, 4966. (d) Marcus, R. A. *Annu. Rev. Phys. Chem.* **1964**, *15*, 155. (e) Marcus, R. A. *J. Chem. Phys.* **1965**, *43*, 679. (f) Waisman, E.; Worry, G.; Marcus, R. A. *J. Electroanal. Chem.* **1977**, *82*, 9. (g) Marcus, R. A. *Faraday Discuss. Chem. Soc.* **1982**, *74*, 7. (h) Marcus, R. A.; Sutin, N. *Biochim. Biophys. Acta* **1985**, *811*, 265.

(4) (a) Sargent, C. D.; Lux, G. A. *J. Am. Chem. Soc.* **1968**, *90*, 7160. (b) Garst, J. F.; Barbas, J. T.; Barton, F. E. *J. Am. Chem. Soc.* **1968**, *90*, 7159. (c) Garst, J. F. *Acc. Chem. Res.* **1971**, *4*, 400. (d) Garst, J. F.; Barton, F. E. *J. Am. Chem. Soc.* **1974**, *96*, 223. (e) Margel, S.; Levy, M. *J. Electroanal. Chem.* **1974**, *56*, 259. (f) Lund, H.; Michel, M. A.; Simonet, J. *Acta Chem. Scand., Ser B* **1974**, *28*, 900. (g) Bank, S.; Juckett, D. A. *J. Am. Chem. Soc.* **1975**, *97*, 567. (h) Garst, J. F.; Abels, B. N. *J. Am. Chem. Soc.* **1975**, *97*, 4926. (i) Sease, W. J.; Reed, C. R. *Tetrahedron Lett.* **1975**, 393. (j) Britton, W. E.; Fry, A. *J. Anal. Chem. USSR* **1975**, *47*, 95. (k) Simonet, J.; Michel, M. A.; Lund, H. *Acta Chem. Scand., Ser B* **1975**, *29*, 489. (l) Bank, S.; Juckett, D. A. *J. Am. Chem. Soc.* **1975**, *97*, 567. (m) Malissard, M.; Mazaleyrat, J. R.; Welvart, Z. *J. Am. Chem. Soc.* **1977**, *99*, 6933. (n) Hebert, E.; Mazaleyrat, J. P.; Welvart, Z.; Nadjo, L.; Savéant, J-M. *Nouv. J. Chim.* **1975**, *9*, 75. (o) Andrieux, C. P.; Gallardo, I.; Savéant, J-M.; Su, K. B. *J. Am. Chem. Soc.* **1986**, *108*, 638. (p) Andrieux, C. P.; Savéant, J-M.; Su, K. B. *J. Phys. Chem.* **1986**, *90*, 3815. (q) Lund, T.; Lund, H. *Acta Chem. Scand., Ser B* **1986**, *40*, 470. (r) Savéant, J-M. *Mechanisms and Reactivity in Organic Electrochemistry. Recent Advances.* Proceedings of the Robert A. Welsh Foundation Conferences on Chemical Research XXX, Advances in Electrochemistry, Houston, TX, 1986; Chapter IV, pp 289–336. (s) Savéant, J-M. *J. Am. Chem. Soc.* **1987**, *109*, 6788. (t) Savéant, J-M. *Bull. Soc. Chim. Fr.* **1988**, 225.

0002-7863/88/1510-7617$01.50/0

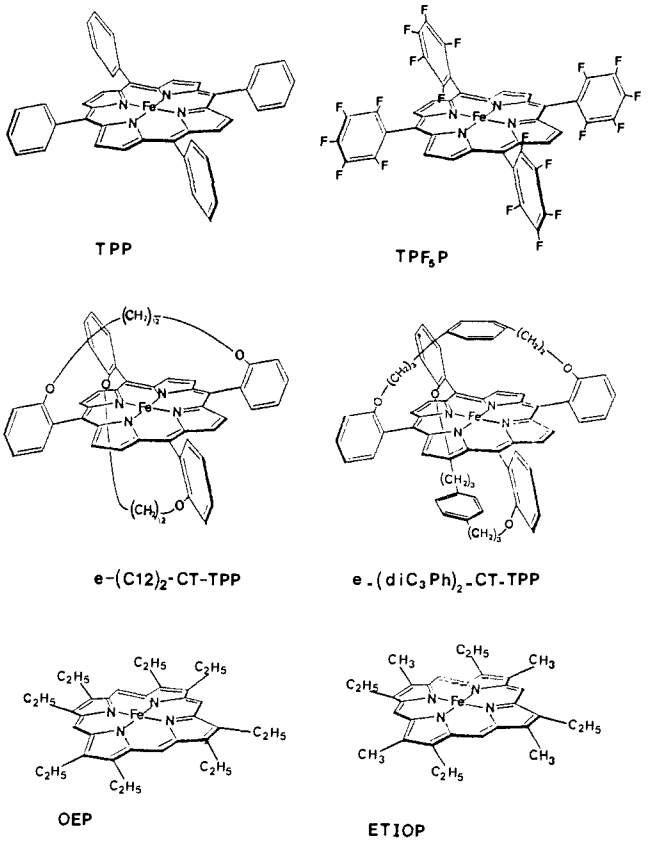

Figure 1. Iron porphyrins investigated in this work (CT designates the cross-trans arrangement of the basket-handle chains).

It should be emphasized that reaction 1 actually possesses an inner-sphere character since it proceeds along a concerted electron transfer–bond breaking mechanism rather than through the intermediacy of an $RX^{\bullet-}$ anion radical.[1a,4o,p,r-t] It is an outer-sphere process from the standpoint of the electron donor but an inner-sphere process from the standpoint of RX. It differs from the S_N2 reaction in the sense that reactions 1 and 2 occurs concertedly in the latter case and not in the former. Evidence supporting a nonbonded transition state for the aliphatic halide–aromatic anion radical reaction comes essentially from the following observations. (i) When generated electrochemically from the parent hydrocarbon, aromatic anion radicals have been observed to give rise, upon reaction with RX, to catalytic currents[1a,4e,f,i-k,o-q] which can be used, through their variations with experimental parameters such as scan rate (in cyclic voltammetry), concentrations of catalyst, and substrate, to investigate the reaction mechanism.[5] This has been shown to proceed along the following reaction scheme:[4o]

$$D + e^- \rightleftarrows D^{\bullet-} \quad (4)$$

$$RX + D^{\bullet-} \rightarrow D + R^{\bullet} + X^- \quad (1)$$

$$R^{\bullet} + D^{\bullet-} \rightarrow R^- + D \quad (5)$$

$$R^{\bullet} + D^{\bullet-} \rightarrow RD^- \quad (3)$$

$$R^{\bullet} + e^- \rightarrow R^- \quad (6)$$

Reactions 5 and 6 produce a catalytic current, whereas complete predominancy of reaction 3 would lead to a two-electron per molecule substitution ($RX + D + 2e^- \rightarrow RD^- + X^-$). In several cases, either complete catalysis or mixed catalysis–substitution

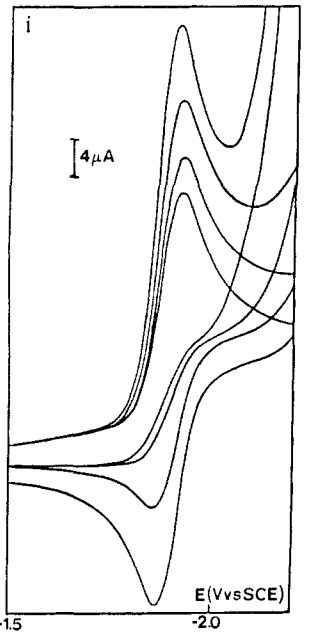

Figure 2. Cyclic voltammetry of 1.14 mM anthracene in DMF + 0.1 M NEt_4ClO_4 at 10 °C at a sweep rate of 0.1 V s^{-1} upon addition of increasing amounts of *t*-BuBr. Concentration of *t*-BuBr (from bottom upward): 0, 0.5, 2, 11.5 mM.

has been shown to operate,[4o] substantiating the conclusion that bond formation occurs in a follow-up step (3) rather than concertedly with the concerted electron transfer–bond breaking step (1 + 2). It does not, however, completely exclude that, in the numerous cases where a two-electron substitution exclusively occurs, the concerted (1 + 2) process may take place at least to a certain extent. (ii) Investigation of the stereochemistry (racemization versus inversion) of the reaction of optically active 2-octyl halides with anthracene anion radical has been the occasion of an early experimental discussion of the outer-sphere electron transfer (ET) versus S_N2 problem in the reaction of aromatic anion radicals with alkyl halides.[4n] It was shown that racemization dominates over inversion (ca. 90% vs. ca. 10%), again indicating that the nonbonded process predominates. The question, however, arises whether the S_N2 process could not be more important, or even predominant, with primary halides where steric hindrance to bond formation is weaker. (iii) A simple modeling of the kinetics of the concerted single electron transfer–bond breaking reaction in polar media has recently been devised[4s] as an extension of Hush–Marcus theory for purely outer-sphere electron transfers.[6] Application to the reduction of alkyl halides by electrogenerated aromatic anion radicals showed a satisfactory adherence of the experimental and theoretical activation versus driving force plots, at least at room temperature.[4s]

It follows that this reaction deserves a closer inspection of the nonbonded character of the transition state. This is one of the

(5) (a) Andrieux, C. P.; Dumas-Bouchiat, J. M.; Savéant, J-M. *J. Electroanal. Chem.* **1978**, *87*, 39. (b) *J. Electroanal. Chem.* **1978**, *87*, 55. (c) *J. Electroanal. Chem.* **1978**, *88*, 27. (d) Andrieux, C. P.; Blocman, C.; Savéant, J-M. *J. Electroanal. Chem.* **1979**, *79*, 413. (e) Andrieux, C. P.; Dumas-Bouchiat, J. M.; Savéant, J-M. *J. Electroanal. Chem.* **1970**, *113*, 1. (f) Savéant, J-M.; Su, K. B. *J. Electroanal. Chem.* **1984**, *171*, 341. (g) Savéant, J-M.; Su, K. B. *J. Electroanal. Chem.* **1985**, *136*, 1. (h) Nadjo, L.; Savéant, J-M.; Su, K. B. *J. Electroanal. Chem.* **1985**, *196*, 23.

(6) (a) Although applied to the reaction of alkyl halides with aromatic anion radicals,[1b,c,4q,6b,c] Hush–Marcus theory of outer-sphere electron transfer is not devised for concerted electron transfer–bond breaking reactions.[4o,p,r-t] Hush–Marcus theory of outer-sphere electron transfer leads to two main results:[3] a quadratic activation–driving force free energy relationship and a standard activation energy being the sum of two terms featuring solvent fluctuational reorganization and bond length and angle reorganization occurring upon electron transfer, respectively. As shown recently,[4s] for concerted electron transfer–bond breaking reactions in polar media, the second term has to be replaced by a bond breaking contribution equal to one-fourth of the bond energy, whereas the solvent reorganization and the reorganization of the bonds that are not broken during the reaction can be estimated as in the theory of outer-sphere electron transfer. The quadratic form of the activation–driving force relationship is retained, based on a Morse curve approximation for the reactants ($RX + e^-$) and a purely dissociative approximation for the products ($R^{\bullet} + X^-$). This model provides a more rigorous approach of the contribution of bond breaking to the intrinsic barrier than previous empirical correlations with the force constant of stretching frequency of the carbon–halogen bond.[4o,p,6d] (b) Eberson, L. *Adv. Phys. Org. Chem.* **1982**, *18*, 79. (c) Eberson, L. *Chem. Ser* **1982**, *20*, 29. (d) Reference 1b, pp 122, 123.

points addressed in the following discussion, based on an investigation of the dependency of the rate constant upon temperature.

On the other hand, there are several cases where compounds usually considered as redox reagents in the sense that they belong to a reversible redox couple, both members of which are chemically stable, do not react as an outer-sphere reagent along a concerted single electron transfer–bond breaking pathway. Early examples of such a behavior were found in the reaction of iron(I) and cobalt(I) porphyrins with *n*-butyl halides[7] as revealed by the measured rate constant being much larger than the value that would be obtained upon reaction of the same RX with an outer-sphere reagent, such as an aromatic anion radical, having the same standard potential.[1a,8a,b] The same strategy has been used more recently with organic anions and dianions as electron donors;[4a,8c-e] with *n*- and *sec*-butyl bromides the reaction is significantly faster than with aromatic anion radicals, whereas the reactivity is about the same with *t*-BuBr and neopentyl bromide.

A large part of the following discussion is devoted to the reaction of iron("0") porphyrins[9] with *n*-, *sec*-, and *t*-BuBr. As shown previously,[9e] the reaction of iron("0") porphyrins with *n*-BuBr yields an iron-alkylated complex as in the case of iron(I) porphyrins. As seen in the following, Fe("0") is more reactive than Fe(I) for the same porphyrin ring, enabling us to investigate more completely the reaction with *sec*- and *t*-BuBr as well as with *n*-BuBr. We also investigated the reaction with neopentyl bromide as another example of a sterically hindered substrate.

In discussing the dichotomy between ET and S_N2 processes, the view has been expressed that ET and S_N2 are the extremes of the same mechanism according to the "degree of concertedness" of bond formation with electron transfer and bond breaking.[2d,4q] How the "degree of concertedness" could control the dichotomy between ET and S_N2 is difficult to understand since, in the first case, bond breaking is concerted with electron transfer, and bond breaking and bond formation are concerted with electron transfer in the second (with no "degree" in concertedness in both cases).[10a] The important factor is the degree of bond formation in the transition state, which, together with the degree of bond breaking, determines the lowering of the transition state energy in the S_N2 case as compared to the ET case. On energy grounds only, ET would thus appear as an extreme of the S_N2 mechanism (corresponding to a vanishingly small bonding stabilization of the transition state) rather than ET and S_N2 being the extremes of the same mechanism. Within this framework, one therefore cannot conceive how competition between the two pathways could occur and how borderline cases or intermediate mechanisms[10b] could exist. These questions will be discussed in the following, based on the comparison of the rate constants obtained with aromatic anion radicals, on one hand, and low oxidation state porphyrins, on the other, as a function of the standard potential, as well as on a temperature dependence investigation for some of these reactants. The latter experiments point to the importance of the energy–entropy balance in the transition state for controlling the competition between the ET and S_N2 pathways. The conclusions suggested by the investigation of these experimental systems are intended to be applicable to the ET–S_N2 problem in general. As such, they thus represent a contribution to the understanding of the more general question of outer-sphere versus inner-sphere electron transfer dichotomy.

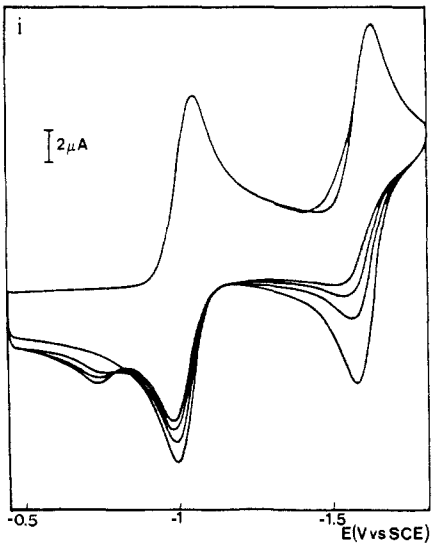

Figure 3. Cyclic voltammetry of 1 mM $TPPFe^{III}Cl$ in DMF + 0.1 M NEt_4ClO_4 at 10 °C in the presence of *t*-BuBr at 0.1 V s^{-1}. Loss of reversibility of the Fe(I)/Fe("0") wave upon addition of *t*-BuBr. BuBr concentration (mM), from bottom upward: 0, 2, 8, 30.

Results

The iron porphyrins investigated in this work are shown in Figure 1 together with their conventional designation.

The room-temperature rate constants of the reaction of the three butyl bromides and of neopentyl bromide with aromatic anion radicals that we will use in the discussion were obtained from previous work.[4o,q] (The data of ref 4o later confirmed by those of ref 4q were used for the butyl bromides and those of ref 4q for neopentyl bromide.)

The reaction with anthracene anion radical was reinvestigated as a function of temperature between 20 and -50 °C. Figure 2 shows typical cyclic voltammograms obtained with anthracene anion radical upon addition of RBr. The initially reversible one-electron wave of anthracene loses its reversibility and increases

(7) (a) The $Fe^{III}R$ and $Co^{III}R$ metal alkylated complexes are obtained as the primary product.[1a] In the case of iron, the $Fe^{III}R$ complex is further reduced into the $Fe^{II}R^-$ complex, since the Fe(II)/Fe(I)$^-$ standard potential is negative to that of the $Fe^{III}R/Fe^{II}R^-$ complex, whereas the opposite is true with cobalt.[1a] (b) For a general discussion of the reduction of the reduction of organic halides by other metal complexes see: (c) Kochi, J. K. *Organometallic Mechanisms and Catalysis*; Academic Press: New York, 1978; Chapter 7.

(8) (a) In several cases, the comparison requires the extension of the Brønsted plot to potentials that are positive to the range where the measurement concerning the outer-sphere reactants were carried out.[1a] Extrapolating then the Brønsted plot with the best fit parabola appears justified in view of the quadratic form of the activation–driving force relationship.[4q] (b) The aforementioned data have been incorporated together with those pertaining to aromatic anion radicals and other low oxidation state complexes into a gross correlation attempting to prove the generality of the outer-sphere pathway,[1c] at variance with the very essence of the demonstration that an inner-sphere pathway is followed with iron(I) and cobalt(I) porphyrins.[1a] This point of view has, however, been revised recently (see ref 1b, pp 118–123). (c) Kinetic data for the reaction of alkyl halides with other organic carbanions (9-substituted fluorenides) have recently appeared.[8d,e] (d) Bordwell, F. G.; Wilson, C. A. *J. Am. Chem. Soc.* **1987**, *109*, 5470. (e) Bordwell, F. G.; Harrelson, J. A. *J. Am. Chem. Soc.* **1987**, *109*, 8112.

(9) (a) The electrochemical reduction of iron(I) to iron("0") (formal oxidation state) in a vast family of simple and superstructured porphyrins has been described elsewhere as a function of electronic and microenvironmental factors leading to an extended range of standard potentials.[9b,c] (b) Lexa, D.; Momenteau, M.; Rentien, P.; Rytz, G.; Savéant, J-M.; Xu, F. *J. Am. Chem. Soc.* **1984**, *106*, 4755. (c) Gueutin, C.; Lexa, D.; Momenteau, M.; Savéant, J-M.; Xu, F. *Inorg. Chem.* **1986**, *25*, 4294. (d) Fe("0") porphyrins, as well as the Fe(I) porphyrins are a combination of resonant forms. In the case of Fe(I) porphyrins, there is little doubt from spectroscopic evidence that the Fe(I) complex is the predominant resonant form (see a discussion of this point in ref 9e and 9f). The case of Fe("0") porphyrins is more ambiguous. Available spectroscopic evidence, however, points to the Fe(I) anion radical as the dominant form.[9e-g] (e) Lexa, D.; Savéant, J.-M.; Wang, D. L. *Organometallics* **1986**, *5*, 1428. (f) Donohoe, R. J.; Atamian, M.; Bocian, D. F. *J. Am. Chem. Soc.* **1987**, *109*, 5593. (g) Reed, C. A. *Adv. Chem. Ser.* **1982**, *No. 201*, 333. (h) Mashiko, T.; Reed, C. A.; Haller, K. J.; Scheidt, W. R. *Inorg. Chem.* **1984**, *23*, 3192. (i) Teraoka, J.; Hashimoto, S.; Sugimoto, H.; Mori, M.; Kitagawa, T. *J. Am. Chem. Soc.* **1987**, *109*, 180. (j) The notation $D^{\bullet-}$ that we use for aromatic anion radical is also suited to the case of iron(I) porphyrins but not quite for iron("0") porphyrins, since they bear a double negative charge and no unpaired electron. The latter will therefore be designated by D^{2-}. Except for a small work term correction of the driving force scale (arising from the electrostatic repulsion of Fe(I)$^-$ and X^-), the whole reasoning is, however, the same as for aromatic anion radicals and iron(I) porphyrins.

(10) (a) In the framework of the Born–Oppenheimer approximation, concertedness means that electron transfer occurs along an appropriate nuclear configuration, involving, besides solvent reorganization and internal vibrations, partial bond breaking (ET, S_N2) and partial bond formation (S_N2). (b) In other words, "gray mechanisms" conceived as an intermediate between "black" and "white" mechanisms (ET and S_N2).[2d]

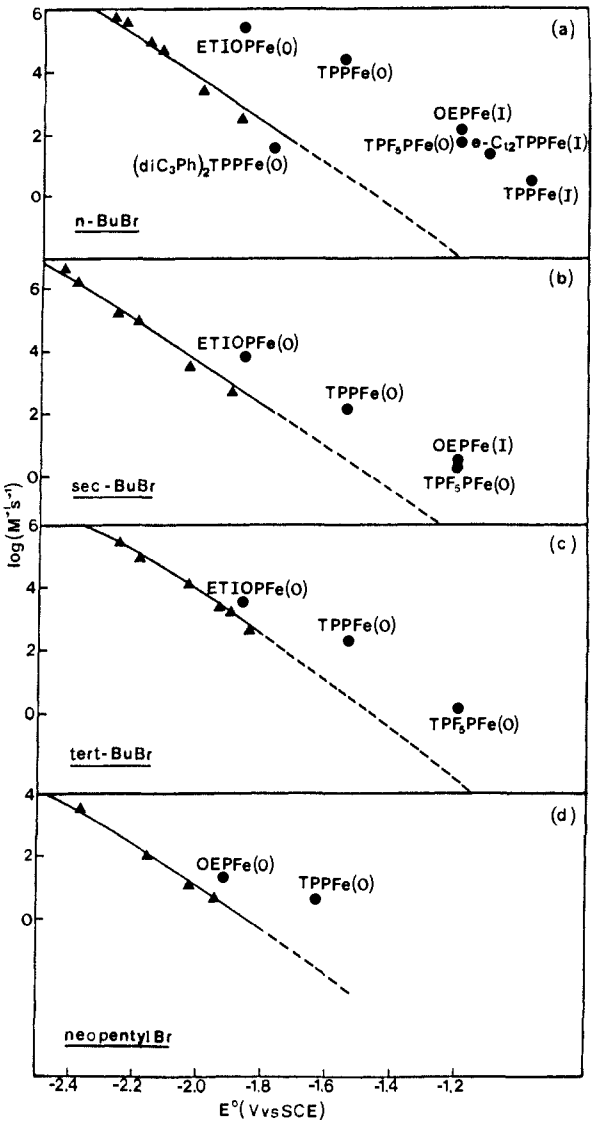

Figure 4. Rate constants of the reaction of iron("0") and iron(I) porphyrins and aromatic anion radicals with *n*-, *sec*-, and *t*-butyl and neopentyl bromides as a function of their standard potentials. Temperature: 20 °C (*n*-Bu and neopentyl), 10 °C (*sec*- and *t*-Bu).

in height up to a two-electron per molecule stoichiometry in accord with the mechanism involving reactions 4, 1, and 3 or reactions 1 + 2 as previously discussed. The rate constant was then derived from the peak current increase according to a procedure described in the Experimental Section.

Starting from an iron(III) porphyrin, the $Fe(II)/Fe(I)^-$ wave exhibits upon addition of *n*-BuBr a behavior similar to that of anthracene.[1a] In addition, a reversible one-electron wave appears upon scan reversal, positive to the $Fe(II)/Fe(I)^-$ wave, featuring the $Fe^{III}R/Fe^{II}R^-$ reversible redox couple.[1a] The rate constant is then obtained along the same procedure as for anthracene.

The behavior exhibited by the $Fe(I)^-/Fe("0")^{2-}$ wave, from which the $Fe("0")^{2-}$ + BuBr rate constants are derived, is different. The initially reversible one-electron $Fe(I)^-/Fe("0")^{2-}$ wave becomes irreversible upon addition of RBr while still corresponding to a one-electron per mole stoichiometry (Figure 3). Upon scan reversal, an anodic wave featuring the oxidation of the $Fe^{II}R^-$ complex formed as the henceforth irreversible $Fe(I)^-/Fe("0")^{2-}$ wave appears. This behavior has been previously observed in the reaction of iron("0") porphyrins with primary halides.[9c] The degree of reversibility of the $Fe^{II}R^-$ oxidation wave and the potential difference between the $Fe(II)/Fe(I)^-$ and $Fe^{III}R/Fe^{II}R^-$ waves depend upon the butyl bromides, featuring the absolute and relative stabilities of the $Fe^{III}R$ and $Fe^{II}R^-$ complexes as described and discussed in detail elsewhere.[11]

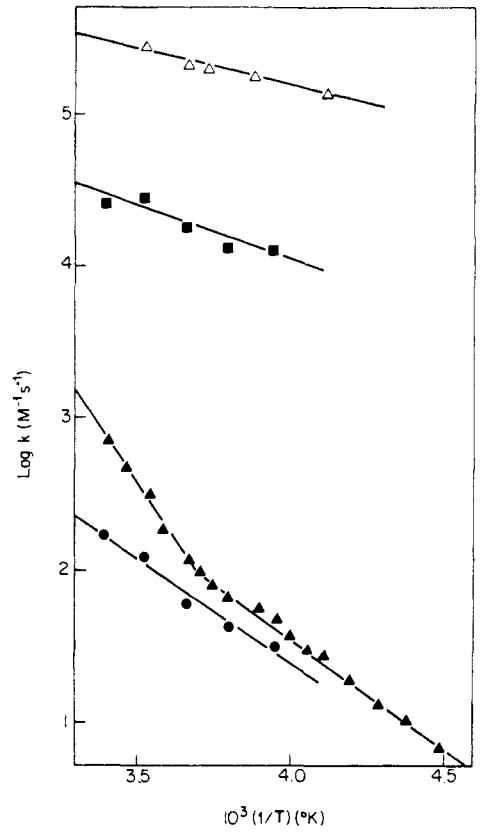

Figure 5. Arrhenius plots for the reaction of *n*-butyl bromide with anthracene anion radical (▲), $ETIOPFe^{"0"}$ (△), $TPPFe^{"0"}$ (■), and $OEPFe^{I}$ (●) (in DMF + 0.1 M NEt_4ClO_4).

The rate constants of the reaction of the Fe("0") porphyrins were obtained from the numerical simulation of the $Fe(II)/Fe(I)^-/Fe("0")^{2-}$ waves (Figure 3), according to an "EEC" mechanism:[12]

$$Fe(II) + e^- \rightleftarrows Fe(I)^- \quad (E)$$

$$Fe(I)^- + e^- \rightleftarrows Fe("0")^{2-} \quad (E)$$

$$Fe("0")^{2-} + RBr \rightarrow Fe^{II}R^- + Br^- \quad (C)$$

However, still another reaction should be taken into account, viz the homogeneous electron transfer coproportionation of $Fe("0")^{2-}$ and Fe(II):

$$Fe("0")^{2-} + Fe(II) \rightarrow 2Fe(I)^-$$

The neglect of this downhill fast reaction, which competes with reaction C, can seriously deteriorate the accuracy of the determination of the alkylation rate constant[13] (the simulation procedure

(11) (a) Gueutin, C.; Lexa, D.; Savéant, J-M.; Wang, D. L. *Organometallics*, submitted. (b) In all cases, however, including *t*-BuBr, the $Fe^{II}R^-$ complex was formed quantitatively upon reacting the iron("0") porphyrins with the butyl bromides. This is also the case for the reaction of *n*-BuBr with the encumbered $e\text{-}(diC_3Ph)_2\text{-}CT\text{-}TPPFe^{"0"}$ porphyrin.

(12) (a) Nicholson, R. S.; Shain, I. *Anal. Chem.* **1964**, *36*, 706. (b) Bard, A. J.; Faulkner, L. W. *Electrochemical Methods*, Wiley: New York, 1980; pp 429–487. (c) Andrieux, C. P.; Savéant, J-M. *Electrochemical Reactions*. In *Investigations of Rates and Mechanisms of Reactions*; Bernasconi, C. F., Ed.; Wiley: New York, 1986; Vol. 6, 4/E, Part 2, pp 305–390.

(13) (a) In spite of its high rate, this reaction has no effect on the current if the three members of the two successive redox couples have the same diffusion coefficient and are not engaged in any other independent reaction.[13b,c] This is obviously not the case here owing to reaction C. One might attempt to circumvent this problem and create a simple EC situation by starting the potential scan at the foot of the $Fe(I)^-/Fe("0")^{2-}$ wave, i.e., from a situation close to that of a pure Fe(I) solution. This is, however, not possible, since during the initial period of the experiment, the $Fe(I)^-$ complex would react with RBr, even though less rapidly than the $Fe("0")^{2-}$ complex, which would affect the height and reversibility of the $Fe(I)^-/Fe("0")^{2-}$ wave, rendering the rate constant determination uncertain. The same problem arises with dianions of aromatic hydrocarbons, but was apparently not taken into consideration.[4q] (b) Andrieux, C. P.; Savéant, J-M. *J. Electroanal. Chem.* **1970**, *28*, 339. (c) Andrieux, C. P.; Hapiot, H.; Savéant, J-M. *J. Electroanal. Chem.* **1984**, *172*, 49.

Table I. Reaction of Butyl Bromides with Anthracene Anion Radical, Iron(0) and Iron(I) Porphyrins: Activation Enthalpies[a] and Entropies[b]

		"ET" Behavior		"S_N2" behavior	
electron donor	BuBr	$\Delta H^{\ddagger}$	$\Delta S^{\ddagger}$	$\Delta H^{\ddagger}$	$\Delta S^{\ddagger}$
anthracene	*n*-	13.6 (±0.6)	5 (±2)	7.0 (±0.2)	−19.1 (±1)
anion	*sec*-	11.4 (±0.9)	−1 (±3)	8.2 (±0.5)	−13 (±2)
radical	*t*-	10.4 (±0.4)	−1.9 (±0.4)	*c*	*c*
ETIOPFe$^{\cdot 0}$	*n*-	*c*	*c*	2.3 (±0.4)	−21 (±2)
	sec-	11 (±2)	4 (±5)	*d*	*d*
	t-	10.0 (±0.5)	−1.7 (±0.4)	*c*	*c*
TPPFe$^{\cdot 0}$	*n*-	*c*	*c*	3.4 (±0.9)	−22 (±3)
OEPFe[I]	*n*-	*c*	*c*	6.5 (±0.8)	−22 (±3)

[a] In kcal/mol. [b] In cal/(mol K). [c] Not observed in the experimentally accessible temperature range. [d] The Arrhenius plot tends to bend upward as the temperature decreases; however, no clearly defined "S_N2" region appears.

is described in the Experimental Section). The rate constants, k, thus derived for the reaction of the various iron("0") and iron(I) porphyrins with *n*-, *sec*-, and *t*-BuBr and neopentyl bromide are displayed in Figure 4 as a function of their standard potential, together with the rate constants obtained with the same substrates and aromatic anion radicals as the electron donor. The solid line is the best fit parabola through the log k points as a representation of the nonbonded concerted electron transfer-bond breaking activation versus driving force–free energy relationship.[6a]

In order to get a better understanding of the reasons for the observed differences in reactivity between iron("0") and iron(I) porphyrins, on one hand, and aromatic anion radicals, on the other, we investigated the temperature dependency of the rate constant for the reaction of ETIOPFe$^{\cdot 0/2-}$ and of the anthracene anion radical, which have almost the same standard potential, with the three butyl bromides. The ensuing Arrhenius plots are shown in Figures 5 and 6.

Arrhenius plots were also investigated for the reaction of *n*-BuBr with another iron("0") porphyrin, TPPFe$^{\cdot 0}$, and with an iron(I) porphyrin, OEPFe[I]. The results are shown in Figure 5.

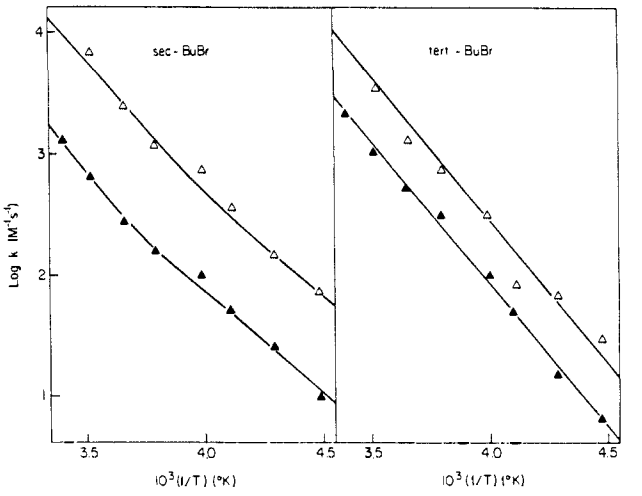

Figure 6. Arrhenius plots for the reaction of *sec*- and *tert*-butyl bromides with anthracene anion radical (▲) and ETIOPFe$^{\cdot 0}$ (△) (in DMF + 0.1 M NEt_4ClO_4).

Discussion

Comparison of the rate constants for the reaction of the three butyl bromides and of neopentyl bromide with iron("0") and iron(I) porphyrins, on one hand, and aromatic anion radicals, on the other (Figure 4), suggests the following remarks. With *n*-BuBr, the rate constant is significantly larger than that of the aromatic anion radical of same standard potential (Figure 4a), pointing to the S_N2 character of the reaction, in all cases but one, viz the *e*-(diC_3Ph)$_2$-CT-TPPFe$^{\cdot 0}$ porphyrin. How the S_N2 character of the process is affected by steric hindrance can be seen in two ways. The effect of steric hindrance at the carbon center is revealed by the fact that, passing from *n*-BuBr to *sec*- and *t*-BuBr, the representive points of the iron("0") and iron(I) porphyrins get significantly closer to the aromatic anion radical line. This is also the case with neopentyl bromide. On the other hand, steric hindrance at the iron center is revealed by the fact that the point representing the reaction of the highly encumbered *e*-(diC_3Ph)$_2$-CT-TPP porphyrin (see Figure 1 and note that the two phenyl groups can rotate freely, thus considerably weakening the bonding interactions in the transition state[11b]) with *n*-BuBr falls right on the aromatic anion radical line, unlike the other, unencumbered, porphyrins.

The variations of the rate constant with temperature (Figures 5 and 6) provide further insights. The Arrhenius plot for anth$^{\cdot -}$ + *n*-BuBr appears as composed of two distinct straight lines of clearly different slopes and intercepts. In the high-temperature range, both slope and intercept are significantly larger than in the low-temperature range. This behavior persists with the anth$^{\cdot -}$ + *sec*-BuBr reaction, although less clearly, the transition being shifted toward low temperatures. With *t*-BuBr, the large slope–large intercept behavior is observed practically in the whole experimentally accessible temperature range.

These observations suggest the existence of two limiting mechanisms with clearly different activation enthalpies and entropies. The values of these are listed in Table I for anth$^{\cdot -}$ as well as for the various iron porphyrins as derived from Figures 5 and 6. The enthalpies were obtained from the slopes of the linear portions of the Arrhenius plots and the entropies from:

$$\ln k = \ln Z - (\Delta H^{\ddagger}/RT) + (\Delta S^{\ddagger}/R)$$

where Z is the collision frequency, estimated from the gas-phase Smoluchovski equation for spherical reactants ($Z = 3 \times 10^{11}$ M^{-1} s^{-1}).[14a] More important than the absolute values of the entropies themselves are, however, the differences between the two entropies for the two limiting behaviors. For the reaction of iron("0") and iron(I) porphyrins with *n*-BuBr, a small activation enthalpy–negative entropy behavior, i.e., similar to the low-temperature behavior of anth$^{\cdot -}$, is observed in all cases. For the reaction of ETIOPFe("0") with *sec*- and *t*-BuBr, the large enthalpy–zero entropy behavior is observed in most of the temperature range, as in the case of anth$^{\cdot -}$.

The following picture thus emerges from these observations. Two limiting mechanisms can operate according to temperature. They can be described as an outer-sphere single electron transfer (concerted with bond breaking) mechanism (ET) and an inner-sphere concerted single electron transfer–bond breaking–bond forming mechanism (S_N2), respectively. ET involves a large activation enthalpy and an activation entropy close to zero.[14b] S_N2 conversely involves a small activation enthalpy and a negative activation entropy of the order of −20 eu. This can be rationalized in the framework of the scheme shown in Figure 7. Among the electron donor molecules that approach the RX molecule, those

(14) (a) This is at best a rough approximation for a liquid-phase reaction. (b) Besides the uncertainties in the evaluation of the Z factor for a liquid-phase reaction, a slightly positive activation entropy could result from the electric charge being less concentrated in the transition state than in the reactants leading to more solvent fluctuation disorder in the transition state. Bending vibration of the C–X bond in the transition state could enhance its partition function and thus contribute to increase the activation entropy. As far as colinear bond reorganization is concerned, we thus assume that the activation entropy is close to zero.

which come to the back of the carbon center with their reacting center aligned, or close to be aligned, with the carbon–halogen bond react with a small activation enthalpy. The stabilization of the transition state, then observed, results from the possibility of partial bond formation together with partial bond breaking. We then have the classical picture of an S_N2 reaction, implying Walden inversion of the carbon substituents. The price to pay, however, is a geometrically ordered transition state leading to a negative activation entropy which tends to slow down the reaction. The electron donor molecules that hit the RX molecules from other directions can still react provided their thermal energy is sufficient to overcome a larger activation barrier, larger because there is no bond formation in the transition state of this concerted single electron transfer–bond breaking reaction[4s] (ET). The bond is then formed in a successive step from coupling with $D^{\bullet}$ (as shown in Figure 7), or more likely with $D^{\bullet-}$ itself in the case of $anth^{\bullet-}$. There is no entropy constraint for such a mechanism and racemization takes place since the $R^{\bullet}$ radical possesses a planar configuration.

In this context, it is remarkable that all S_N2 activation entropies for the reaction with *n*-BuBr fall around the same value, −20 to −25 eu. A rough estimation of the entropy difference for an aligned and nonaligned transition state gives a value of −18 eu[15] in keeping with the above model. The activation enthalpy in the S_N2 process is smaller than in the ET process because of bond formation in the transition state. In this connection, the driving force for the S_N2 process (i.e., concerted electron transfer–bond breaking–bond forming reaction) is no longer (ET):

$$E^{\circ}_{RX/R\bullet+X^-} - E^{\circ}_{D/D\bullet-} = E^{\circ}_{X\bullet/X^-} - E^{\circ}_{D/D\bullet-} - \Delta G^{\circ}_{RX/R\bullet+X\bullet}$$

or

$$E^{\circ}_{RX/R\bullet+X^-} - E^{\circ}_{D\bullet^-/D^{2-}} = E^{\circ}_{X\bullet/X^-} - E^{\circ}_{D\bullet^-/D^{2-}} - \Delta G^{\circ}_{RX/R\bullet+X\bullet}$$

but rather (S_N2):

$$E^{\circ}_{RX/R\bullet+X^-} - E^{\circ}_{RD\bullet/R\bullet+D\bullet^-} = E^{\circ}_{X\bullet/X^-} - E^{\circ}_{D/D\bullet^-} - \Delta G^{\circ}_{RX/R\bullet+X\bullet} + \Delta G^{\circ}_{RD\bullet/R\bullet+D}$$

or

$$E^{\circ}_{RX/R\bullet+X^-} - E^{\circ}_{RD^-/R\bullet+D^{2-}} = E^{\circ}_{X\bullet/X^-} - E^{\circ}_{D\bullet^-/D^{2-}} - \Delta G^{\circ}_{RX/R\bullet+X\bullet} + \Delta G^{\circ}_{RD^-/R\bullet+D\bullet^-}$$

(15) (a) The calculation was carried out from (see Chapters IV and V in ref 15b):

$$\frac{A_{S_N2}}{A_{ET}} = \frac{I^{\ddagger}_{S_N2}}{I_{RX} I^{\ddagger}_{ET}} \frac{h^2}{8\pi^2 kT}$$

the *A*'s being the preexponential factors relating to the entropy variations by $A = \exp(-\Delta S^{\ddagger}/RT)$ and the *I*'s the respective moments of inertia. These are given by (the *m*'s and the *d*'s are the corresponding masses and distances):

$$I^{\ddagger}_{ET} = \frac{m_D m_{RX}}{m_D + m_{RX}} (d^{\ddagger}_{D\text{-}RX})^2$$

in which RX is considered as approximately spherical and $d^{\ddagger}_{D\text{-}RX}$ is the distance between the equivalent RX and D spheres.

$$I^{\ddagger}_{S_N2} = \frac{m_D(m_R + m_D)(d^{\ddagger}_{DR})^2 + 2m_D m_R (d^{\ddagger}_{DR} d^{\ddagger}_{RX}) + m_X(m_D + m_R)(d^{\ddagger}_{RX})^2}{m_D + m_R + m_X}$$

$$I_{RX} = \frac{m_R m_X}{m_R + m_X} (d_{RX})^2$$

in which RX is no longer considered as spherical (see Figure 7), $d^{\ddagger}_{DR}$, $d^{\ddagger}_{RX}$ being the distances between the centers of the D and R and R and X equivalent spheres in the transition state and d_{RX} the bond distance in the starting RX molecule. In the case of anthracene and *n*-BuBr, the anthracene and *n*-BuBr equivalent sphere average radii were taken as 3.35 and 3.66 Å, respectively. For the anthracene–C and C–Br partial bond lengths in the S_N2 transition state, we took 1.97 Å as a common guessed value. Small variations of these lengths do not affect the final result to a large extent. It was thus deemed to be of the same order of magnitude for the iron porphyrins. (b) Glasstone, S.; Laidler, K. J.; Eyring, H. *The Theory of Rate Processes*, McGraw-Hill: New York, 1941; pp 190, 193, 213.

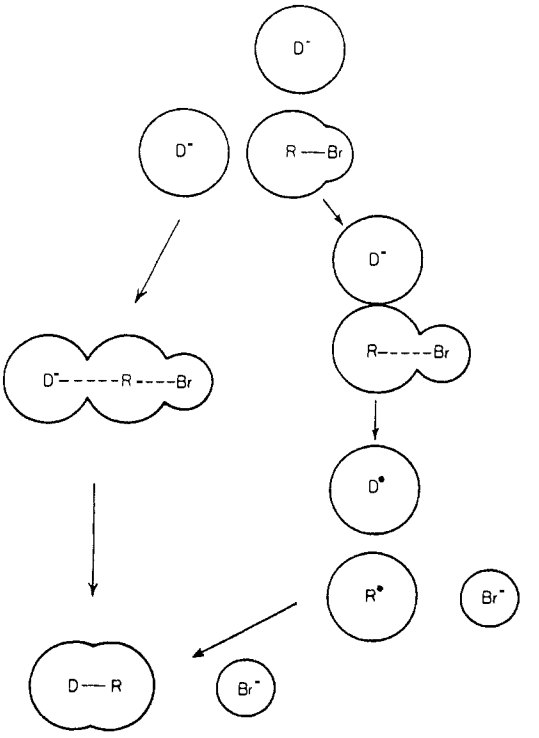

Figure 7. Schematic picture of the ET and S_N2 mechanisms.

Even for only this reason, the activation energy of S_N2 process is smaller than that of the ET process.[16] In addition, the intrinsic barrier (activation energy at zero driving force) is also lower, due to partial bond formation in the transition state.

Two other points are worth noting in this connection. The log *k* points for the reaction of the unencumbered iron("0") and iron(I) porphyrins with *n*-BuBr are approximately located on a common line, descending as the standard potential increases. This suggests that within this particular series of nucleophiles, the variation of the driving force is mainly caused by the variation of the standard potential rather than by that of the bond energy of the σ-alkyl–iron bond in the final product. Likewise, the decrease of the intrinsic barrier caused by bonding interactions in the zero driving force transition state does not seem to vary much in the series. With sterically encumbered alkyl bromides, the most positive iron("0") and iron(I) porphyrins have a rate constant still significantly above the outer-sphere line, suggesting that non-negligible bonding interactions take place in the transition state in spite of steric hindrance. Replacement of the ET-S_N2 pathway by bromine or bromonium abstraction cannot, however, be totally exlcuded (Br abstraction is, however, not plausible for Fe("0") since there is no driving force for forming $Fe^{I}Br^{2-}$).

Iron("0") porphyrins are extremely easy to oxidize (E° in the range −1 to −2 V vs. SCE) as compared to classical nucleophiles such as, for example, OH^- ($E^{\circ} \simeq 0.5$ vs. SCE in DMF[17]). They, nevertheless, react along an S_N2 mechanism rather than an ET mechanism in the whole accessible temperature range, at least in the absence of steric constraints. Bond formation in the transition state thus allows a gain of 2–4 orders of magnitude in rate constant. With a hard, arduously oxidizable, nucleophile such as OH^-, bonding interactions in the transition state ought to be much stronger for the reaction to proceed at a significant rate (the rate constant for the reaction of OH^- with *n*-BuBr along an ET mechanism would be of the order of 10^{-22} M^{-1} s^{-1}, based on the activation–driving force relationship shown in Figure 4 and on a rough estimation of the $OH^{\bullet}/OH^-$ standard potential[17]).

(16) (a) Marcus cross-reaction free energy relationship has been shown to be approximately followed in the "methyl transfer" reactions,[16c] i.e., S_N2 substitutions at an aliphatic carbon.[16b] (b) Albery, W. J.; Kreevoy, M. M. *Adv. Phys. Org. Chem.* **1978**, *15*, 87. (c) Actually methyl cation transfer reactions.

Experimental Section

Chemicals. The DMF and butyl and neopentyl bromides, from commercial origin, were distilled before use. Et_4NClO_4 (Fluka purum) was used as supporting electrolyte. It was recrystallized twice before use in a 3:1 ethyl acetate–ethanol mixture. The TPPFeCl, TPF_5PFeCl, OEPFeCl porphyrins were from commercial origin (Alfa, Aldrich) and used as received. The ETIOFeCl porphyrin was prepared by insertion of iron into the free base (Sigma).[18] The *e*-$(diC_3Ph)_2$TPPFeCl porphyrin was provided by M. Momenteau. It was prepared and characterized as described in ref 19.

Electrochemical Measurements. An inactinic double-wall Pyrex cell, suitable for the analysis of 5-mL solutions, was used throughout the work. Methanol was circulated between the cell jacket and a Huber cryothermostat so as to fix the temperature of the solution at any desired value between +20 and −50 °C with an accuracy of ±1 °C. The working electrode was a glassy carbon disk of 3-mm diameter, carefully polished and ultrasonically rinsed in ethanol before use. The counter electrode was a platinum wire. The reference electrode was a DMF Cd(Hg)/$CdCl_2$ electrode[20] thermostated at 20 °C. It is 630 mV negative to the aqueous SCE at the same temperature (to which all potentials are referred). Cyclic voltammograms were obtained using an home-built potentiostat and current measurer equipped with a positive feedback ohmic drop compensation,[21] a Parr (175) function generator, and a X–Y chart recorder (IFELEC 2502).

Procedures for Determination of Rate Constants. The rate constants were derived from the changes of the cyclic voltammetric wave corresponding to the generation of the electron donor upon addition of the alkyl bromide to the solution. The concentration of anthracene or iron porphyrin was in the millimolar range, and the excess of alkyl bromide over the electron donor, γ, was varied so as to obtain the maximal accuracy as described below. The measurements were carried out at three different scan rates, 0.05, 0.10, 0.20 V s^{-1}, in most cases.

In the case of $anth^{\bullet-}$ and iron(I) porphyrins, the wave of interest changes from a 1e/molecule reversible behavior to a 2e/molecule irreversible behavior upon increasing RX concentration (Figure 2). The cyclic voltammograms corresponding to the following mechanism were thus simulated:

$$P + e \rightleftarrows Q$$

$$Q + A \xrightarrow{k} B + \text{products}$$

$$Q + B \rightarrow P + \text{products}$$

The kinetics is indeed the same for the set of reactions 1–3 whether (1) and (2) are concerted or not, provided, as seems reasonable, that the steady-state assumption applies for $R^{\bullet}$. The last reaction is expected to be fast, since it is a downhill outer-sphere electron transfer reaction. The steady-state assumption can therefore be applied to B as well. The partial derivative equations system with the accompanying boundary and initial conditions to be solved is thus:

$$\frac{\partial p}{\partial \tau} = \frac{\partial^2 p}{\partial y^2} + \lambda a q$$

$$\frac{\partial q}{\partial \tau} = \frac{\partial^2 q}{\partial y^2} - 2\lambda a q$$

$$\frac{\partial a}{\partial \tau} = \frac{\partial^2 a}{\partial y^2} - \lambda a q$$

$$\tau = 0,\ \gamma > 0 \text{ and } \gamma = \infty,\ \tau > 0:\ p = 1,\ q = 0,\ a = \gamma$$

$$y = 0,\ \tau > 0:\ p = q \exp[-F/RT(E - E^\circ)],\ \partial a/\partial y = 0$$

with $E = E_i - vt$

where p, q, a are the P, Q, A concentrations normalized toward the bulk concentration of P; $\tau = Fvt/RT$ is a dimensionless time normalized toward the sweep rate; v, $y = x(DRT/Fv)^{1/2}$, a dimensionless space variable (x: distance from the electrode surface), normalized toward the diffusion layer thickness; E is the electrode potential, E_i the initial potential of the scan, and E° the standard potential of the anth/$anth^{\bullet-}$ or of Fe(II)/$Fe(I)^-$ couple; γ is the excess of alkyl halide over the electron donor; and $\lambda = RTkC_p^\circ/Fv$, a dimensionless rate parameter normalizing the reaction toward the scan rate. The dimensionless current $i/FSC_p^\circ D^{1/2}(Fv/RT)^{1/2}$ is then equal to $\partial p/\partial y$ for $y = 0$. The numerical calculations were carried out using the Crank–Nicholson finite difference technique.[22]

When the excess factor, γ, is large, in practice larger than 10, a can be considered as constant and equal to γ. The overall kinetics is thus the same as for a DISP1 reaction scheme[12c,23] and depends upon a single parameter, $\lambda\gamma$. The determination of k was then carried out using an i_p/i_p° (peak current in the presence and in the absence of RBr, respectively) vs. $\lambda\gamma$ working curve by linear interpolation between two close values of $\lambda\gamma$, for each value of v and γ. k is then derived from the equation defining λ. The standard deviation thus found for k was then of the order of 10–15%.

For smaller excess factors, i_p/i_p° is a function of two parameters, λ and γ, and all three partial derivative equations have to be numerically solved simultaneously. A working curve is then computed for each value of γ. The standard deviation was then found to be of the same order of magnitude as above.

As the temperature decreases, the charge transfer kinetics of the P/Q couple tends to interfere, albeit slightly, in the cyclic voltammetry of the electron donor in the absence of alkyl bromide as revealed by an increase of the cathodic to anodic peak separation over the Nernstian value.[12b,c] In order to see if this influences also the cyclic voltammetry in the presence of butyl bromide and therefore affects the rate constant determination, we repeated the simulations for the lower edge of the temperature range, taking this factor into account. This implies the replacement of the Nernst law in the above $y = 0$ boundary conditions by the Volmer–Butler law, obtaining the standard rate constant for the electrode electron transfer to P from the cathodic to anodic peak separation of the wave obtained in the absence of alkyl bromide. It was thus shown that this factor has a negligible influence on the rate constant determination.

In the case of iron("0") porphyrins, we start from a system of two successive one-electron reversible waves, Fe(II)/$Fe(I)^-$/$Fe(0)^{2-}$, the second of which becomes irreversible upon addition of the butyl bromide (Figure 3). The cyclic voltammograms corresponding to the following mechanism were thus stimulated:

$$P + e \rightleftarrows Q$$

$$Q + e \rightleftarrows S$$

$$S + A \xrightarrow{k} \text{products}$$

$$S + P \xrightarrow{k'} 2Q$$

the kinetics being, indeed, the same whether reactions 1 and 2 are concerted or not for the same reasons as discussed in the preceding case. The partial derivative equations, boundary and initial conditions set to be solved is now:

$$\frac{\partial p}{\partial \tau} = \frac{\partial^2 p}{\partial y^2} - \lambda' p s \qquad \frac{\partial q}{\partial \tau} = \frac{\partial^2 q}{\partial y^2} + 2\lambda' p s \qquad \frac{\partial s}{\partial \tau} = \frac{\partial^2 s}{\partial y_2} - \lambda s a - \lambda' p s$$

$$\frac{\partial a}{\partial \tau} = \frac{\partial^2 a}{\partial y^2} - \lambda s a$$

$$\tau = 0,\ y > 0 \text{ and } y = \infty,\ \tau > 0:\ p = 1,\ q = s = 0,\ a = \gamma$$

$$y = 0,\ \tau > 0:\ p = q \exp[-F/RT(E - E^\circ_1)],$$

$$q = s \exp[-F/RT(E - E^\circ_2)] \text{ with } E = E_i - vt$$

where the symbols have the same meaning as before (with $\lambda' = RTk'C_p^\circ/Fv$, s being the normalized concentration of S), E°_1 and E°_2 being the standard potentials of the two successive redox couples. The dimensionless current $i/FSC_p^\circ D^{1/2}(Fv/RT)^{1/2}$ is now equal to $(\partial p/\partial y) - (\partial s/\partial y)$ for $y = 0$. The observable that we simulate is the anodic current of the second wave as measured at the standard potential of the second wave (E°_2) from the value of the current at the inversion potential

(17) (a) From ref 17b–e. (b) *Handbook of Chemistry and Physics*, 52nd ed.; CRC: Cleveland, 1972; p E95. (c) Wagman, D. D.; Evans, W. H.; Parker, V. B.; Schumm, R. H.; Halow, I.; Bailey, S. M.; Churney, K. L.; Nuttal, R. L. *J. Phys. Chem. Ref. Data* **1982**, *11*, Suppl. 2. (d) Cos, B. G.; Hedwig, G. R.; Parker, A. J.; Watts, D. W. *Aust. J. Chem.* **1976**, *27*, 677. (e) Koppenol, W. H.; Liebman, J. F. *J. Phys. Chem.* **1984**, *88*, 89.

(18) Baudreau, C. A.; Caughey, W. S. *Biochemistry* **1968**, *7*, 624.

(19) Momenteau, M.; Mispelter, J.; Look, B.; Bisagni, E. *J. Chem. Soc., Perkin Trans. 1* **1983**, 183.

(20) Marple, L. W. *Anal. Chem.* **1967**, *39*, 865.

(21) Garreau, D.; Savéant, J-M. *J. Electroanal. Chem.* **1972**, *35*, 309.

(22) Crank, J. *Mathematics of Diffusion*; Oxford University Press: London, 1957.

(23) Amatore, C.; Gareil, M.; Savéant, J-M. *J. Electroanal. Chem.* **1983**, *147*, 1.

taken as a baseline. The inversion potential was set 200 mV negative to E°_2 in all cases. The observable is a function of two parameters, viz λ and λ'. We observed that in the useful range of λ values (i.e., in-between 0.01 and 1) the observable versus λ working curve tends toward a limit as λ' increases. This limit is reached within 1% as soon as λ' is equal to 100. The S + P reaction being a strongly downhill process, k' is close to the diffusion limit, and therefore λ' is much larger than 100 in all practical situations. On the other hand, the numerical calculations required more and more computer time and accuracy as λ' increases. We therefore carried out all the simulations taking $\lambda' = 100$. A systematic comparison of the observable versus λ working curves for $\lambda' = 0$ and $\lambda' = 100$ revealed that the error on k determination resulting from the neglect of the S + P → 2Q reaction would be larger than 100% in most cases.

Conclusion

The main conclusions that emerge from the above discussion of the ET–S_N2 problem as illustrated by the reactions of aromatic anion radicals, iron("0") and iron(I) porphyrins with alkyl bromides, are as follows.

The ET pathway is characterized by a large activation enthalpy and a close to zero activation entropy. For an electron donor having the same standard potential, the S_N2 pathway is characterized by a small activation enthalpy and a substantially negative entropy.

As far as energy alone is concerned, the S_N2 process is always more favorable than the ET pathway since the transition state is stabilized by partial bond formation. The more so, the more favored the S_N2 over the ET pathway and vice versa. One reason for this is the increase in driving force accompanying bond formation in the immediate product of the reaction since the S_N2 pathway is to be viewed as an elementary step in which bond formation is concerted with electron transfer and bond breaking whereas the ET pathway involves only concerted electron transfer and bond breaking in the rate-determining step, bond formation occurring in a second successive step. In addition to this, there is a decrease of the intrinsic barrier (viz. activation energy at zero driving force). For obvious reasons, steric hindrance to bond formation resulting from an encumbered carbon center, and/or an encumbered electron donor reacting center, diminishes and eventually annihilates the energetical auspiciousness of the S_N2 pathway over the ET pathway.

As discussed in the introduction, it is not possible to conceive competition, borderline cases, or intermediate mechanisms on activation energy grounds only. ET would appear as a limiting case of S_N2, when the stabilization of the transition state is so weak as to produce a negligible effect on the rate constant (0.1 kcal for an accuracy of 15% on rate constant determination at room temperature). One could still say that one S_N2 reaction is closer to ET, or has less S_N2 character, than another S_N2 reaction (for example, the reaction of *n*-BuBr with iron("0") or iron(I) porphyrins as compared to OH^-) but this would simply mean that bonding interactions in the transition state, although present in both cases, would be less in the first than in the second case.

Activation energy considerations are, however, only one facet of the problem. On entropy grounds, the S_N2 pathway is disfavored in comparison with the ET pathway due to a geometrically more ordered transition state leading to an entropy difference on the order of 20 eu against the S_N2 pathway in the absence of steric constraints. Through the enthalpy–entropy balance, we now understand what is the factor that may determine the transition from the S_N2 pathway to the ET pathway, namely, *temperature*. High temperatures favor the ET pathway; conversely, low temperatures favor the S_N2 pathway. The temperature of transition depends upon the extent of the energetical advantage of the S_N2 pathway over the ET pathway and the difference in activation entropies. If bonding interactions in the transition state are strong, the S_N2 pathway will be followed in the whole accessible temperature range, the ET pathway requiring too high a temperature to appear (this is the case for reactions of iron("0") and iron(I) porphyrins with *n*-BuBr). Conversely, if the bonding interactions in the transition state are weak, owing, e.g., to steric hindrance, the ET pathway will be followed in most of the accessible temperature range, the S_N2 pathway requiring too small a temperature to appear (this is the case for the reaction of $anth^{\bullet -}$ and of the iron("0") porphyrins with *t*-BuBr). Note in this connection that when bonding interactions in the transition state become vanishingly small, not only the activation enthalpies but also the activation entropies of ET and S_N2 merge. A typical borderline example is the reaction of $anth^{\bullet -}$ with *n*-BuBr where the ET and S_N2 pathways are followed at the upper and lower edges of the accessible temperature range, respectively. Along the same lines one may now understand why, at room temperature, the reaction of $anth^{\bullet -}$ with optically active 2-octyl halides, while leading mostly to racemization (ca. 90%), shows a small but significant amount of inversion (ca. 10%).

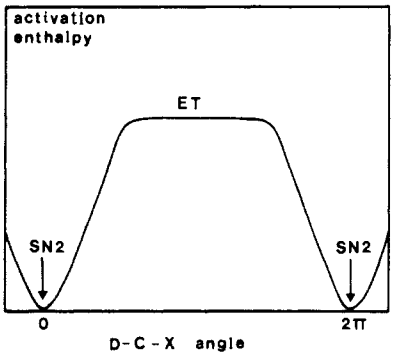

Figure 8. Schematic representation of the variations of the activation enthalpy with the D–C–X angle.

Are the ET and S_N2 pathways the extremes of a common mechanism?[4q] How can we conceive their competition?[4n] Is there the possibility of an S_N2–ET mechanistic spectrum?[2c]

As discussed above, these questions cannot be meaningfully answered on activation energy grounds only. Simultaneous consideration of energy and entropy factors allows the following answers. For the ET pathway the coordinates of the potential energy hypersurface should represent solvent reorganization, vibrations of the bonds not broken in the reaction and the carbon-leaving group distance. They are the same for the S_N2 pathway with, in addition, the carbon–electron donor distance. If we wish to view the S_N2 and ET pathways as belonging to the same potential energy hypersurface, we need to introduce an additional coordinate, namely, the D–C–X angle (in the framework of a revolution symmetry around the C–X axis). Figure 8 sketches the variations of the activation enthalpy with the D–C–X angle. More precisely, for each value of the D–C–X angle, the ordinate is the value of the potential energy minimized toward the other coordinates. The bottom and top of the curve then represent the limiting pathways, S_N2 and ET, respectively, while the rising and descending portions represent intermediate types of transition states. These different activated complexes have different geometries. There is, therefore, a spectrum of different activation energies and entropies. Thus upon raising temperature the system will tend to pass from an S_N2 to an ET situation. Whether or not the temperature for the transition falls in the experimentally accessible range is a function of the relative values of the activation enthalpies and entropies:

$$T_{\text{transition}} = (\Delta H^{\ddagger}_{ET} - \Delta H^{\ddagger}_{S_N2})/(\Delta S^{\ddagger}_{ET} - \Delta S^{\ddagger}_{S_N2})$$

The sharpness of the transition depends upon the involvement of the intermediate activated complexes: the more abrupt the rising (and descending) portions of the activation enthalpy versus D–C–X angle curve, the sharper the transition. The reaction of $anth^{\bullet -}$ with *n*-BuBr offers a typical example of a sharp transition clearly observable within the accessible temperature range.[24] Other transitions are observed when steric hindrance to bonding interactions in the transition state increases, both because the energy gap is less and intermediate transition states may be more heavily involved. For example, with *sec*-BuBr and iron porphyrins,[24] some

(24) To the best of our knowledge, this, with the reaction of *sec*-BuBr with $anth^{\bullet -}$, is the first experimental examples of a transition between the ET and S_N2 pathways, clearer in the first case than in the other two.

bonding interaction may exist for D–C–X angles different from zero, as results from an optimal fit between this large and flat reactant and the back of the carbon center which bears substituents of unequal bulkiness.

The preceding analysis also allows one to formulate with more precision the assumption underlying the recently developed model of concerted electron transfer–bond breaking reactions.[4s] A purely dissociative potential energy curve was assumed for the products ($R^\bullet + X^-$), considering that the $R^\bullet$, X^- complex possibly resulting from induced dipole ($R^\bullet$) charge (X^-) interaction was destabilized by solvation of X^- in a polar solvent. This is not necessarily true, since a weak complex may be formed between RX and the electron donor molecules that attack the carbon center in the axis of the C–X bond.[25] For the other electron donor molecules, i.e., those reaching in an ET manner, such a complex should not be formed and purely dissociative $R^\bullet + X^-$ potential energy curve is in order, thus supporting the proposed model.[4s]

Another question, related to the above discussion, concerns the possible relationship between single electron transfer and S_N1 substitution. In the framework of the following reaction scheme:

$$RX \rightleftarrows R^+ + X^- \quad (7)$$

$$R^+ + D^- \rightarrow R^\bullet + D^\bullet \quad (8)$$

$$R^\bullet + D^\bullet \rightarrow RD \quad (9)$$

the classical S_N1 mechanism corresponds to steps 8 and 9 being concerted, meaning that electron transfer involves partial bond formation in the transition state. It is, however, conceivable that reactions 8 and 9 can be sequential. An extreme example of such a behavior can be found in the reaction of 9-chloro-9-mesitylfluorene with electrogenerated outer-sphere reagents (ferrocene, substituted ferrocenes, anion radicals of chloranil, tetracyanoethylene, tetracyanoquinodimethane, dichlorodicyanobenzoquinone).[26a] Since the $R^\bullet$ radical is strongly resonance stabilized, reaction 9 does not occur. The rate-determining step is then reaction 7 and the overall kinetics is independent of the standard potential of electron donor in the aforementioned series except for the dichlorodicyanobenzoquinone anion radical. Although reaction 7 is a strongly uphill process, reaction 8 is so fast[26b] that it prevents backward reaction 8 from occurring.[26c] With stronger homogeneous reducing agents as well as in the case of the direct electrochemical reduction, the reaction does not proceed via prior formation of the carbocation but rather along a direct electron transfer–bond breaking mechanism of the type discussed above.[26a,d]

$S_{RN}1$ aromatic nucleophilic substitution[4r,t,27] is another example of a substitution reaction in which single electron transfer plays a quite important role. This role is, however, not the same as in the reaction discussed above. The electrophile is indeed not the starting aromatic halide but rather the aryl radical obtained upon sequential outer-sphere electron transfer from an external electron source[28] and bond breaking of the ensuing anion radical. The reaction involves the following sequence of elementary steps:

$$RX + e^- \rightleftarrows RX^{\bullet-} \quad (10)$$

$$RX^{\bullet-} \rightarrow R^\bullet + X^- \quad (11)$$

$$R^\bullet + \text{⟩}^- \rightarrow RD^{\bullet-} \quad (12)$$

$$RD^{\bullet-} - e^- \rightarrow RD \quad (13)$$

The aryl radical then reacts with the nucleophile yielding the anion radical of the substituted product which gives back an electron to the electrode or to RX.[29] The reaction is thus an outer-sphere electron transfer catalyzed process unlike the substitution reactions discussed above.[28] On the other hand, as discussed elsewhere,[30] reactions 11 and 12 can be viewed as intramolecular electron transfers concerted with bond breaking and with bond formation, respectively.

Acknowledgment. Dr. M. Momenteau (Institut Curie, Orsay, France) is gratefully acknowledged for the gift of samples of the *e*-$(C12)_2$-CT-TPP and *e*-$(diC_3Ph)_2$CT–TPP FeCl porphyrins. One of the authors (J.-M.S.) wishes to thank the California Institute of Technology for his selection as a Sherman Fairchild Distinguished Scholar for the period during which the present work was completed.

Registry No. TPP, 16591-56-3; TPF_5P, 79231-62-2; e-$(C12)_2$-CT-TPP, 70196-65-5; e-$(diC_3Ph)_2$-CT-TPP, 70196-66-6; OEP, 61085-06-1; ETIOP, 14566-50-8; *t*-BuBr, 507-19-7; *n*-BuBr, 109-65-9; *sec*-BuBr, 78-76-2; anthracene anion radical, 34509-92-7; neopentyl bromide, 630-17-1.

(25) Symons, M. C. R. *Pure Appl. Chem.* **1981**, *53*, 223.

(26) (a) Andrieux, C. P.; Merz, A.; Savéant, J-M.; Tomahogh, R. *J. Am. Chem. Soc.* **1984**, *106*, 1957. (b) Owing to the easy reducibility of R^+, reaction 9 is a strongly downhill process (driving force >0.35 eV). (c) The dichlorodicyanobenzoquinone anion radical is an example of mixed kinetic control by reactions 8 and 9, owing to a smaller driving force for the electron transfer step (0.2 eV). (d) Andrieux, C. P.; Merz, A.; Savéant, J-M. *J. Am. Chem. Soc.* **1985**, *107*, 6097.

(27) (a) Bunnett, J. F. *Acc. Chem. Res.* **1978**, *11*, 413. (b) Savéant, J-M. *Acc. Chem. Res.* **1980**, *13*, 323. (c) Rossi, R. A. *Acc. Chem. Res.* **1982**, *15*, 161. (d) Rossi, R. A.; Rossi, R. H. *Aromatic Nucleophilic Substitution by the $S_{RN}1$ Mechanism*, ACS Monograph 178; The American Chemical Society: Washington, D.C., 1983.

(28) "Thermal" $S_{RN}1$ processes, i.e., reactions in which the initiating electron (step 10) would come from the nucleophile, and not from an electron donor impurity, have not been characterized unambiguously. The mechanism of the photochemical stimulation of the reaction, although not known with certainty, seems to involve the excitation of a nucleophile–RX complex. In any case, however, the key step of the reaction appears to involve the attack of the nucleophile on the aryl radical (12) rather than the coupling of the aryl radical with the radical that would result from the extraction of one electron from the nucleophile as indicated sometimes.[2c]

(29) Initiating, in the latter case, a chain process.

(30) See ref 4p,r,t and references cited therein.